Gradual localization of *5f* states in orthorhombic UTX ferromagnets – polarized neutron diffraction study of Ru substituted UCoGe

Michal Vališka[1], Jiří Pospíšil[1,2], Anne Stunault[3], Yukiharu Takeda[4], Beatrice Gillon[5], Yoshinori Haga[2], Karel Prokeš[6], Mohsen M. Abd-Elmeguid[7] Gwilherm Nénert[3], Tetsuo Okane[4], Hiroshi Yamagami[4,8], Laurent Chapon[3], Arsène Goukassov[5], Allain Cousson[5], Etsuji Yamamoto[2] and Vladimír Sechovský[1]

[1]*Charles University in Prague, Faculty of Mathematics and Physics, Department of Condensed Matter Physics, Ke Karlovu 5, 121 16 Prague 2, Czech Republic*
[2]*Advanced Science Research Center, Japan Atomic Energy Agency, Tokai, Ibaraki, 319-1195, Japan*
[3]*Institut Laue Langevin, 71 Avenue des Martyrs, CS 20156, F-38042 Grenoble Cedex 9, France*
[4]*Condensed Matter Science Division, Quantum Beam Science Directorate, Japan Atomic Energy Agency, 1-1-1 Kouto, Sayo-cho, Sayo-gun, Hyogo 679-5148, Japan*
[5]*Laboratoire Léon Brillouin, UMR12 CEA-CNRS, Bât 563 CEA Saclay, 91191 Gif sur Yvette Cedex, France*
[6]*Helmholtz-Zentrum Berlin für Materialien und Energie, Hahn-Meitner Platz 1, D-14109 Berlin, Germany*
[7]*Universität zu Köln, II. Physikalisches Institut, Zülpicher Str. 77, 50937 Köln, Germany*
[8]*Department of Physics, Kyoto Sangyo University, Motoyama, Kamigamo, Kita-Ku, Kyoto 603-8555, Japan*

We report on microscopic study of evolution of ferromagnetism in the Ru substituted ferromagnetic superconductor (FM SC) UCoGe crystallizes in the orthorhombic TiNiSi-type structure. For that purpose, two single crystals with composition $UCo_{0.97}Ru_{0.03}Ge$ and $UCo_{0.88}Ru_{0.12}Ge$ have been prepared and characterized by magnetization, AC susceptibility, specific heat and electrical resistivity measurements. Both compounds have been found to order ferromagnetically below T_C = 6.5 K and 7.5 K, respectively, which are considerably higher than T_C (= 3 K) of the parent compound UCoGe. The higher values of T_C are accompanied by enhanced values of the spontaneous moment $\mu_{spont.}$ = 0.11 μ_B/f.u. and $\mu_{spont.}$ = 0.21 μ_B/f.u., respectively in comparison to the tiny spontaneous moment of UCoGe (about $0.07 \mu_B$/f.u.). No sign of superconductivity was detected in both single crystals. The magnetic moments of the samples were investigated on microscopic scale using polarized neutron diffraction (PND) and for $UCo_{0.88}Ru_{0.12}Ge$ also by soft X-ray magnetic circular dichroism (XMCD). The analysis of the PND results indicates that the observed enhancement of ferromagnetism is mainly due to the growth of the orbital part of uranium 5f moment μ_L^U, reflecting a gradual localization of the 5f electrons with Ru substitution. In addition, the parallel orientation of the U and Co moments has been confirmed in both substituted compounds. The results are compared and discussed with related isostructural ferromagnetic UTX compounds (T - transition metals, X – Si, Ge) in the context of a varying degree of the 5f-ligand hybridization.

Key words: UCoGe, URuGe, $UCo_{1-x}Ru_xGe$, ferromagnetism, superconductivity, XMCD, polarized neutron diffraction, PND

PACS numbers: 75.30.Gw, 71.27.+a, 25.40.Dn, 78.70.Dm

I.   Introduction

Uranium magnetism represents a unique part of condensed matter physics and the recent discovery of uranium ferromagnetic superconductors (FM SC) keeps these materials on the top of scientific interest. The group of the uranium FM SC contains to date three members - UGe_2[1] under pressure, $URhGe$[2] and $UCoGe$[3] at ambient pressure. In particular, URhGe and UCoGe have attracted much attention in recent years because they show the coexistence of weak long-range ferromagnetic order and superconductivity at ambient pressure. The investigation of the magnetic field and pressure phase diagrams indicates that these compounds are located near a magnetic instability, suggesting that superconductivity in this class of materials is mediated by critical spin fluctuations associated with a ferromagnetic quantum critical point[3].

Generally, magnetism of uranium intermetallic compounds is determined by a sensitive balance between the direct $5f$-$5f$ interaction described by the Hill limit[4] and overlap of the $5f$ orbitals with ligand s, p and d states of surrounding ions ($5f$-ligand hybridization)[5]. Thus, such complex and sensitive balance leads to unusual magnetic behavior and novel ground states. This is well manifested in the isostructural and simultaneously isoelectronic compounds UCoGe and URhGe: They do not belong to the same Ising type universality class for FM transitions although both are strongly uniaxial ferromagnets[6]. Moreover, they are characterized by distinct difference in their response to hydrostatic pressure as increasing pressure destabilizes[7, 8] and stabilizes[9, 10] the FM state of UCoGe and URhGe, respectively.

Another quite particular magnetic feature is the observed stabilization of the originally very weak itinerant FM by the substitution of the Co(Rh) site by other transition metals even when the opposite side parent compound is a paramagnet[11-13]. As a result, an unusual FM domes exist in $UCo_{1-x}T_xGe$[13, 14] (T = Ru, Fe) and also in $URh_{1-x}T_xGe$[15, 16] (T = Ru, Co) T-x phase diagrams. The observed FM domes are characterized by an increase of the Curie temperature T_C or spontaneous magnetic moment $\mu_{spont.}$ with increasing initial substitutions. The development of ferromagnetism in substituted $UCo_{1-x}T_xGe$[13, 14] and $URh_{1-x}T_xGe$[15, 16] has a serious impact on superconducting state, as it is immediately suppressed already by few percent of substituent element[11]. This implies drastic changes of the ferromagnetic state and magnitude of spin fluctuations in the substituted systems. The complexity of the behavior is underlined by recent studies of the $UCo_{1-x}T_xGe$ and $URh_{1-x}T_xGe$ systems substituted with Fe or Ru showing that FM domes vanish around 20-40 % of substituent accompanied by development of a non-Fermi liquid (NFL) behavior[13, 15, 17]. However, so far there is no detailed microscopic study to explore the origin of such drastic changes both in ferromagnetism and superconductivity in the $UCo_{1-x}T_xGe$ and also $URh_{1-x}T_xGe$ systems.

In this respect, we want to mention that the FM state of parent UCoGe is rather complex as Co exhibits a moment and thus significantly contributes to total ordered magnetic moment. Therefore, UCoGe has been the subject of recent experimental[18-22] and theoretical[23, 24] efforts: especially PND experiments on UCoGe at 0.1 K and magnetic field of 12 T predicted an induced moment on the Co site that compares to the uranium moment and is antiparallel to it[21]. From this point of view a ferrimagnetic state is predicted in UCoGe in high magnetic fields[19]. As a matter of fact, the reported antiparallel polarization of the Co magnetic moment to the direction of the U magnetic moment, however, contradicts with the behavior found in related so far studied ferromagnetic UTX (X = Al, Ga, Si, Ge) compounds, for which the U and T moments are always found to be parallel, e.g. $URhSi$[25], $UCoAl$[26, 27], $URhAl$[28], $URuAl$[29]. Indeed, recent studies using synchrotron radiation (X-ray magnetic circular dichrorism[30, 31] and Compton scattering[24]) provide strong evidence that the magnetic state of UCoGe is not anomalous and a common ferromagnetic state was found, i.e. total magnetic moments on U and Co are parallel.

In the present work, we have investigated the evolution of the FM state of Ru substituted UCoGe using PND for the first time to inspect the origin of the observed dome like shape of the T-x phase diagram UCo$_{1-x}$Ru$_x$Ge. In particular, we have prepared and characterized two substituted UCoGe single crystals with compositions UCo$_{0.97}$Ru$_{0.03}$Ge and UCo$_{0.88}$Ru$_{0.12}$Ge, by magnetization, AC susceptibility, specific heat and electrical resistivity measurements. PND experiments allows us to gain insight into the microscopic mechanism that stands behind the anomalous increase of the magnetic moment and T_C[32]. We, then try to generalize the results to related isostructural ferromagnetic UTX compounds (T- transition metals, X – Si, Ge) with similar dome-like behavior. We further have performed XMCD measurements on UCo$_{0.88}$Ru$_{0.12}$Ge single crystal to confirm the orientation of U and Co moments determined by PND.

II. Experimental details

Single crystals were prepared using initial stoichiometric amounts of the pure elements (U-Solid State Electrotransport treated[33], Co 3N5, Ge 6N, Ru 3N5). Rather large UCo$_{0.97}$Ru$_{0.03}$Ge and UCo$_{0.88}$Ru$_{0.12}$Ge single crystals (diameter 5 mm, length 3-5cm) were grown for PND by floating zone method in an optical mirror furnace (model: FZ-T-4000-VI-VPM-PC made by Crystal System Corp. For the XMCD measurements, a somewhat smaller UCo$_{0.88}$Ru$_{0.12}$Ge crystal (diameter 2-3 mm, length 5 cm) was grown by Czochralski method in a tetra-arc furnace (Techno Search Corp.), using 99.9% purity U. All the as grown single crystals were wrapped in a Ta foil (purity 4N), sealed in a quartz tube under 10^{-6} mbar vacuum and annealed at 1100 °C for 1 day, then slowly cooled down to 880 °C where they remained for 14 days and finally cooled down to room temperature[34]. The quality and composition of the single crystals were checked by EDX analysis (electron microscope (SEM) Tescan Mira I LMH equipped with energy dispersive X-ray detector Bruker AXS) and Laue method. A small part of each single crystal was grinded and crystal structure was determined by room temperature X-ray powder diffraction using a Bruker D8 Advance diffractometer. The powder X-ray diffraction patterns were evaluated by Rietveld analysis[35] using the FullProf[36]/WinPlotr[37] programs. Several properly shaped samples were extracted from the ingots for the individual measurements using fine wire saw (South Bay Technology 810) to prevent additional stresses. Bar-shaped samples (1 mm x 1 mm x 4 mm) were used for the low temperature resistivity measurements performed in the PPMS14T (Quantum Design) with the ^{3}He insert down to the 350 mK. Heat capacity measurements have been performed on thin plates (2 mm x 2 mm x 0.2 mm) using relaxation method in the same PPMS9T and PPMS14T devices using ^{3}He insert, as well. The magnetization was measured on roughly cubic samples (2mm x 2mm x 2mm) in a MPMS7T device (Quantum Design). The same cubic samples were also used for the neutron diffraction experiments. First, we have performed an experiment with unpolarized neutrons on UCo$_{0.88}$Ru$_{0.12}$Ge single crystal at the four circle hot neutron diffractometer D9 (ILL, Grenoble) and UCo$_{0.97}$Ru$_{0.03}$Ge single crystal at the 5C2 diffractometer (LLB, Saclay), then with polarized neutrons on the same samples at the D3 instrument (ILL, Grenoble)[38] and 5C1 diffractometer (LLB, Saclay). For the XMCD experiments, a clean surface of the UCo$_{0.88}$Ru$_{0.12}$Ge sample was obtained by fracturing in ultra-high vacuum. The experiments were carried out at the U N$_{4,5}$ and the Co L$_{2,3}$ edges at the SPring-8 BL23SU beamline[39].

II. Experimental results

A. Magnetization, electrical resistivity and specific heat

The magnetization measurements of the two substituted samples (Fig. 1) reveal that the c-axis is the easy magnetization direction while a and b axis are the hard ones similar to Ising-like UCoGe. Although the a and b axis are considered as the magnetically hard ones both in UCoGe and URhGe, the ab plane is not magnetically isotropic and the larger moment is always measured along the b axis refereed as intermediate axis[20]. An important feature is that the magnetic behavior of the a and b axis is almost identical in case of the highly substituted $UCo_{0.88}Ru_{0.12}Ge$ sample.

The maximum in the AC susceptibility data and the first derivative of the low field thermomagnetic curves measured in magnetic fields applied along the c-axis point to $T_C = 6$ K and 8.5 K for the $UCo_{0.97}Ru_{0.03}Ge$ and $UCo_{0.88}Ru_{0.12}Ge$, respectively, which are in good agreement with the previous study of polycrystalline samples[32]. We also have estimated the values of T_C from the analysis of the Arrott plots[40] and obtained the same results.
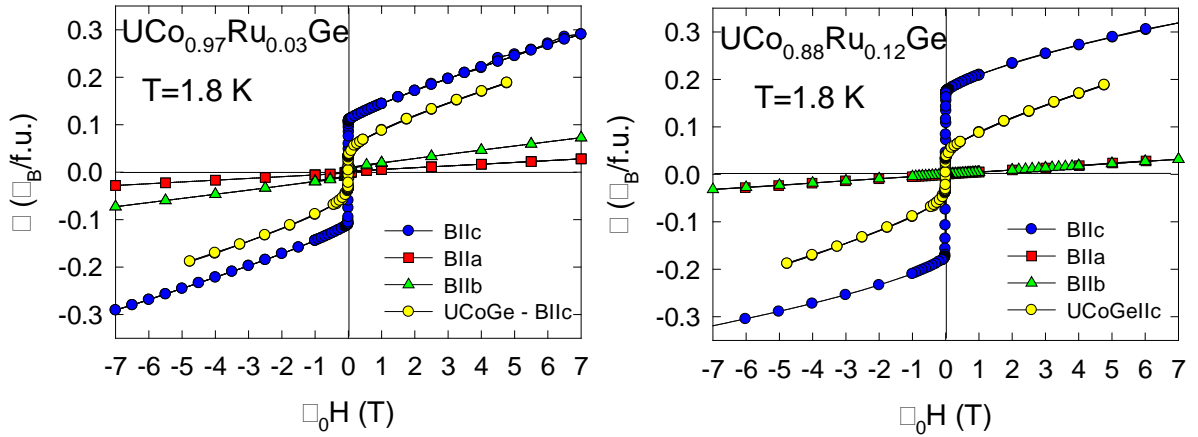

FIG. 1. (Color online) Magnetization loops for the $UCo_{0.97}Ru_{0.03}Ge$ (left), $UCo_{0.88}Ru_{0.12}Ge$ (right) single crystals. The magnetization loop of the parent UCoGe is taken from Ref.[33] is also included for comparison. Magnetization data along the a and b axis overlap for the $UCo_{0.88}Ru_{0.12}Ge$.

The shape of the magnetization loops along the easy axis also shows a clear evolution with the Ru substitution from the soft ferromagnetic behavior of UCoGe to a more rectangular behavior (gradually lower high-field susceptibility) which has been observed in the URhGe[41] or URhSi[42]. The magnetic moment of UCoGe grows continuously with no sign of saturation even in 53 T. This was attributed to still-unquenched magnetic fluctuations and/or a crystal-field splitting[20]. We, thus, suggest that significantly frozen magnetic fluctuations of U moment are responsible for the observed rectangular shape of magnetization loops of substituted compounds. The spontaneous magnetic moment $\mu_{spont.}$ considerably increases from 0.07 μ_B/f.u.in UCoGe to 0.11 μ_B/f.u. in $UCo_{0.97}Ru_{0.03}Ge$ and 0.21 μ_B/f.u. in $UCo_{0.88}Ru_{0.12}Ge$. $UCo_{0.88}Ru_{0.12}Ge$ is close to the optimum concentration where the maximum T_C and $\mu_{spont.}$ is achieved in the $UCo_{1-x}Ru_xGe$ system[32]. Consequently, the hysteresis increases from the initial value of ~4 mT for UCoGe up to ~5.8 mT in $UCo_{0.88}Ru_{0.12}Ge$.

The electrical resistivity along the c axis shows a pronounced maximum at about ~40 K as in UCoGe[33, 43] (Fig. 2). The maximum well coincides with T^* found by NMR study where longitudinal FM fluctuations develop along the c-axis[43]. The maxima in substituted systems seem to be weaker and broaden in comparison to UCoGe. Because the maxima is still conserved high magnetic field experiment is desired to check behavior analogous to above mentioned high magnetic field properties of UCoGe. Electrical resistivity data also exhibit an anomaly corresponding to the Curie temperature with a shoulder at 6.5 and 7.7 K for $UCo_{0.97}Ru_{0.03}Ge$ and $UCo_{0.88}Ru_{0.12}Ge$, respectively.

It is also apparent from Fig. 2 that increasing Ru concentration yields more substitutional disorder in the crystal lattice which consequently leads to reduction of RRR (residual resistivity ratio). This is consistent with the results reported for polycrystalline $UCo_{1-x}Ru_xGe$[14] and $UCo_{1-x}Fe_xGe$[13] samples. The disorder responsible for the low RRR can be of crystallographic and/or magnetic origin. We did not detect any sing of superconductivity even in $UCo_{0.97}Ru_{0.03}Ge$ single crystal down to temperature 0.35 K.
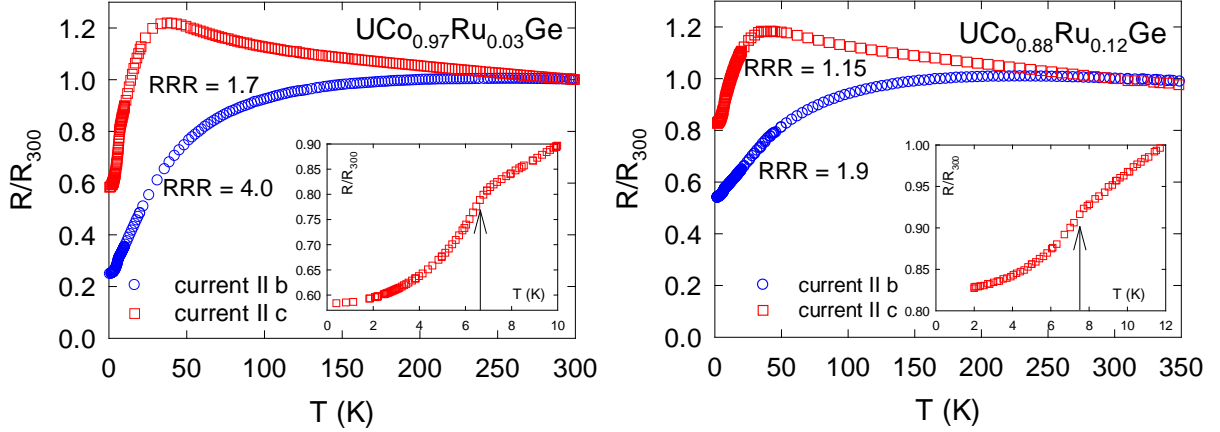

FIG. 2. (Color online) Temperature dependence of the electrical resistivity measured along the b and c axes of the $UCo_{0.97}Ru_{0.03}Ge$ (left) and $UCo_{0.88}Ru_{0.12}Ge$ (right) single crystals. The insets show the low temperature region, arrows point to the anomaly at T_C.

The transition to the FM state is also well documented by the anomaly in the specific heat (Fig. 3). The deduced T_C values of 6.5 and 7.5 K for the $UCo_{0.97}Ru_{0.03}Ge$ and $UCo_{0.88}Ru_{0.12}Ge$, respectively are in agreement with those obtained from the results of magnetic and resistivity measurements. We have analyzed the γ coefficients from the low-temperature specific heat data by linear extrapolation of the C_p/T vs T^2 to 0 K. The obtained value of 64 mJ/molK^2 for $UCo_{0.97}Ru_{0.03}Ge$ is slightly higher than that of UCoGe (57 mJ/molK^2)[3]. Much enhanced value of 79 mJ/molK^2 was estimated in the case of $UCo_{0.88}Ru_{0.12}Ge$. Similar enhancement of the γ coefficients was detected in the heat capacity behavior of $URh_{1-x}Ru_xGe$ and explained by XPS[44] due to an enlargement of the DOS at E_F due to enhanced $5f$-$4d$ hybridization. Stabilization of ferromagnetism with increasing Ru concentration can also be deduced from the growth of the jump at the FM transition observed in the heat capacity data (Fig. 3) and the associated increase of the magnetic entropy from $S_{mag} = 0.06Rln2$ to $S_{mag} = 0.12Rln2$ for $UCo_{0.97}Ru_{0.03}Ge$ and $UCo_{0.88}Ru_{0.12}Ge$, respectively. The behavior of the heat capacity will be further discussed in detail later in relation to other related TiNiSi-type UTX compounds.
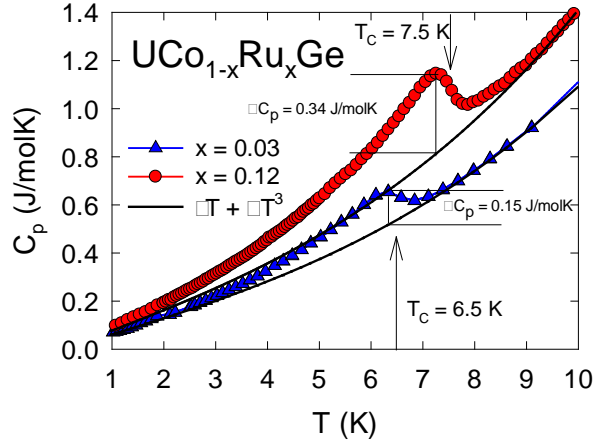
FIG. 3. (Color online) Temperature dependence of the heat capacity of the $UCo_{0.97}Ru_{0.03}Ge$ and $UCo_{0.88}Ru_{0.12}Ge$ single crystals. The arrows mark the Curie temperatures.

B. Polarized neutron diffraction (PND)

Since the macroscopic measurements of $UCo_{0.97}Ru_{0.03}Ge$ and $UCo_{0.88}Ru_{0.12}Ge$ gave similar results, only the experiments on the latter compound will be detailed here. PND is a powerful technique which can give valuable information about the spin density within the unit cell. Since the technique consists in measuring of the flipping ratios, an accurate knowledge of the crystal structure is compelling to extract reliable magnetic structure factors. In the case of $UCo_{0.88}Ru_{0.12}Ge$ the structure was determined at 11 K (i.e. above the T_C) from the measurement of over 350 non-equivalent reflections at the D9 diffractometer of the ILL. The measured integrated intensities were analyzed using the FullProf[36]/WinPlotr[37] software using anisotropic extinction corrections. A comparison of the squares of the measured and calculated intensities is plotted in Fig. 4 showing very good agreement of the measured and calculated values.
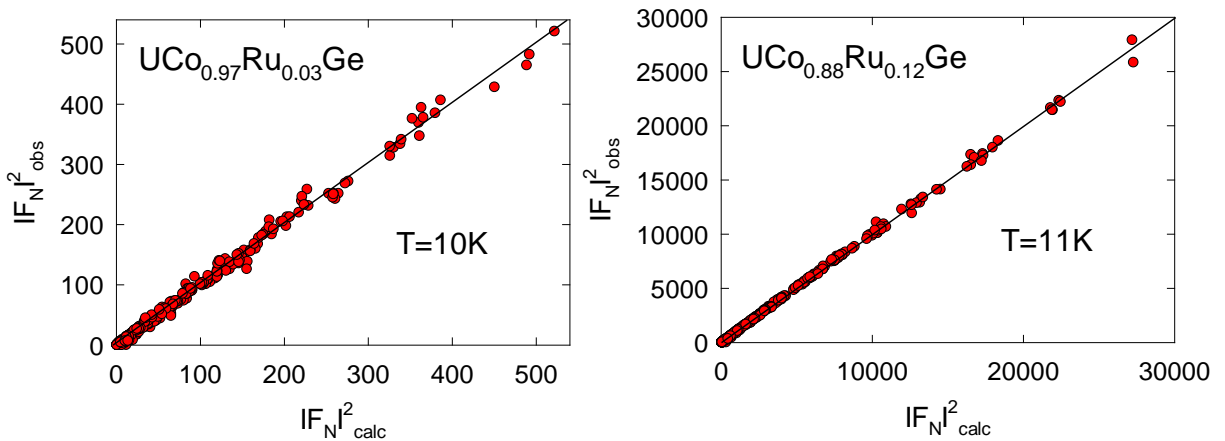

FIG. 4. (Color online) Comparison of the measured and calculated square intensities. Data were taken at the 5C-2 diffractometer of the LLB at 10 K in the case of $UCo_{0.97}Ru_{0.03}Ge$ and at the D9 diffractometer of the ILL at 11 K in the case of $UCo_{0.88}Ru_{0.12}Ge$.

The data refinement confirms that both compounds crystalize in the orthorhombic TiNiSi-type structure like the parent compound[45]. The fit also confirms that Co and Ru share

only the characteristic transition metal *4c* site. The fitted Ru concentration, $x = 13.4 \pm 0.8\%$ of Ru is statistically consistent with the nominal value. Obtained cell parameters together with the fraction coordinates are listed in the Table I and II.

TABLE I. Unit cell parameters of the $UCo_{0.97}Ru_{0.03}Ge$ $UCo_{0.88}Ru_{0.12}Ge$ single crystals.

Composition	Space group	a (Å)	b (Å)	c (Å)	Volume (Å^3)
$UCo_{0.97}Ru_{0.03}Ge$	Pnma	6.8437(6)	4.2097(4)	7.2400(9)	208.583
$UCo_{0.88}Ru_{0.12}Ge$	Pnma	6.7998(3)	4.2104(2)	7.2744(4)	208.265

TABLE II. Evaluated fraction coordinates of the $UCo_{0.97}Ru_{0.03}Ge$ and $UCo_{0.88}Ru_{0.12}Ge$ single crystals from neutron diffraction data. Coefficients of the extinction parameter $q(hkl) = q_1h^2+q_2k^2+q_3l^3+q_4hk+q_5hl+q_6kl$ are listed as well.

$UCo_{0.97}Ru_{0.03}Ge$	x (r.l.u.)	y (r.l.u.)	z (r.l.u.)	occ.
U	0.01051(8)	0.25000	0.70623(9)	1
Co	0.28708(29)	0.25000	0.41677(32)	0.964 (8)
Ru	0.28708(29)	0.25000	0.41677(32)	0.036 (8)
Ge	0.19351(12)	0.25000	0.08695(11)	1
Displacement temp. factors	β_{11}	β_{22}	β_{33}	β_{13}
U	5.1(9)	22(3)	7(1)	-0.5(1)
Co	24(3)	25(9)	11(3)	-0.4(2)
Ru	24(3)	25(9)	11(3)	-0.4(2)
Ge	10(1)	27(3)	11(1)	0.3(2)
Extinction correction	q_1=0.31(4)	q_2=0.6(1)	q_3=0.12(2)	$q_{4,5,6}$=0

$UCo_{0.88}Ru_{0.12}Ge$	x (r.l.u.)	y (r.l.u.)	z (r.l.u.)	occ.
U	0.01031(7)	0.25000	0.70547(8)	1
Co	0.28375(23)	0.25000	0.41618(24)	0.866(8)
Ru	0.28375(23)	0.25000	0.41618(24)	0.134(8)
Ge	0.19239(8)	0.25000	0.08648(9)	1
Displacement temp. factors	β_{11}	β_{22}	β_{33}	β_{13}
U	5(1)	25(3)	10(1)	-0.7(2)
Co	22(5)	30(10)	11(3)	2(1)
Ru	22(5)	30(10)	11(3)	2(1)
Ge	13(1)	27(3)	10(1)	2.0(8)
Extinction correction	q_1=0.29(3)	q_2=0.39(4)	q_3=-0.27(4)	$q_{4,5,6}$=0

The polarized neutron diffraction experiment, carried out at the D3 diffractometer was performed at 1.65 K, well below the ordering temperature and in magnetic fields of 1 T and 9 T applied along the *c* axis. Flipping ratios were collected up to $\sin\theta/\lambda = 0.9$ Å.

Spin densities were deduced from the obtained magnetic structure factors by a maximum entropy calculation by utilization of the MaxEnt software[46-48]. The data refinement followed the same procedure like that in Ref.[21]. The whole unit cell was divided into the 50 x 50 x 50 = 125000 smaller cells before the computation of the distribution of the magnetic moments. The reconstructions were started from a flat magnetization distribution with a total moment in the unit cell equal to the bulk magnetization measured experimentally at the same temperatures in magnetic field. The result (i.e. magnetization density maps with the highest probability) is plotted in the Fig. 5.
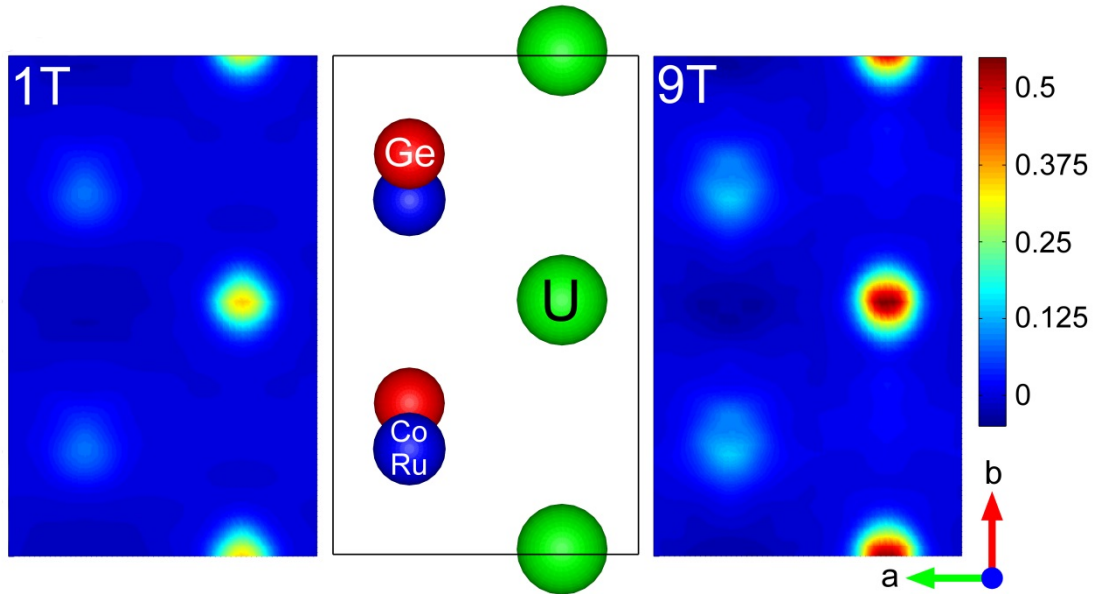

FIG. 5. (Color online) Magnetization density maps for $UCo_{0.88}Ru_{0.12}Ge$; projections onto the *a-b* plane in applied magnetic fields of 1 T and 9 T. The scale of the map is in $\mu_B/\mathring{A}^2$ unit.

The projection of a half of the unit cell to the *a-b* plane is the most illustrative interpretation of the magnetization distribution. The Co magnetic moments are clearly oriented parallel with the U moments in both compounds, which is opposite to the result reported on the parent $UCoGe$[21].

We have integrated the magnetization densities in a defined volume to estimate the absolute value of the magnetic moments centered on these ions. For this purpose we choose the simple spheres centered on the atomic positions. The results of this integration are summarized in the Table III.

In order to obtain information about the spin and orbital component of the magnetic moment of each atom we employed the spin density model. This model works on the basis of the dipolar approximation and its fitting was done using the FullProf[36]/WinPlotr[37] software. Our model involves the magnetic moments born at the U and Co ions. The spherical integrals for both possible ionic states of uranium (U^{3+} and U^{4+})[49] are similar, which disqualifies this method for the determination of the valence of the U ion. For Co ion we took into account only the spin part of the magnetic moment. We have also tried to include a magnetic density on Ru ion but obtained values of the magnetic moments showed significant relative error of more than 250%. Nevertheless, we obtained a positive magnetic density both on the U and Co(Ru) sites. The dipolar approximation also confirmed the expected anti-parallel alignment of orbital μ_L^U and spin μ_S^U component of the U moment. μ_L^U is parallel to the moment at the

Co(Ru) site. All quantities obtained from dipole approximation are summarized in the Table III.

TABLE III. Components of the magnetic moment on the U and Co(Ru) positions from the refinement of the polarized neutron diffraction data of the $UCo_{0.97}Ru_{0.03}Ge$ and $UCo_{0.88}Ru_{0.12}Ge$ single crystals. *Values obtained from the integration of the magnetization density maps using the maximum entropy method and **values from the spin density model on the basis of the dipole approximation using FullProf[36]/WinPlotr[37] software.

composition	$\mu_0 H$	μ_L^U	μ_S^U	$\mu_{tot.}^U$	$\mu_{S.}^{Co}$	$\mu_{tot.}$
$x = 0.03$*	7 T			0.09(1)	0.017(3)	0.11(1)
$x = 0.03$**	7 T	0.23(3)	-0.12(3)	0.11(1)	0.025(8)	0.13(2)
$x = 0.12$*	1 T			0.11(1)	0.07(1)	0.18(2)
$x = 0.12$**	1 T	0.280(6)	-0.15(1)	0.13(2)	0.051(6)	0.18(3)
$x = 0.12$*	9 T			0.26(3)	0.08(1)	0.34(4)
$x = 0.12$**	9 T	0.457(7)	-0.20(1)	0.25(2)	0.069(7)	0.32(3)

We have tested the parallel orientation of the U and Co moments found by PND using XMCD. The XMCD spectrum of $UCo_{0.88}Ru_{0.12}Ge$ was obtained in the ferromagnetic state at $T = 5.5$ K and $H = 10$ T. In the $UCo_{0.88}Ru_{0.12}Ge$ simple XMCD study is difficult to estimate a quantitative value of the magnetic moments by applying the sum rules[50, 51] due to the overlap of the spectra at the U- N_4 and the Co L_3 edges. However, the directions of the orbital and spin magnetic moments can be determined only from the shape of the XMCD spectrum. We have found that integrals of the XMCD intensity at the Co L_3 and L_2 edges are negative and positive, respectively. According to the sum rules, the XMCD spectrum of $UCo_{0.88}Ru_{0.12}Ge$ clearly indicates that the direction of the magnetic moment at U site is parallel to that at the Co site in the ferromagnetic state, which is consistent with the results obtained by the present PND experiment. It should be noted that the orientation between the U and Co sites is the same as that of UCoAl[27]. Detail $UCo_{0.88}Ru_{0.12}Ge$ and UCoGe XMCD spectra analysis will be subject of another specialized article.

IV.   Discussion

In the following we discuss the general trends responsible for behavior of TiNiSi-type UTX ferromagnets and focus on the anomalous development of ferromagnetic domes in the T-x phase diagrams of the substituted systems. This is based on the analysis of the PND data which allowed us to resolve the macroscopic magnetization into contributions from each ion and thereby analyze the microscopic origin of ferromagnetism. We have carried out PND experiments on the two Ru substituted UCoGe samples and performed detail analysis of the data in combination with the results obtained from our macroscopic measurements of the heat capacity, magnetization and electrical resistivity to support our finding and corresponding interpretation.

The distribution of the density of the magnetic moment was obtained from the maximum entropy method, showing that the majority of magnetic moment is located on the uranium site, while a weak induced moment parallel to uranium is detected on the transition metal site-see values in Table III and Fig. 5. The existence of magnetic moment on U and Co site with parallel orientation was confirmed by a soft X-ray XMCD measurement performed on $UCo_{0.88}Ru_{0.12}Ge$ single crystal. PND data analysis did not allow separation of magnetism of Ru ions from Co. Also XMCD signal from the Ru $M_{2,3}$ edge is practically undetectable and most likely denotes that the contribution from Ru ion to total magnetism is rather low.

In a second step, the magnetic form factor on the uranium site has been decomposed into orbital μ_L^U and spin μ_S^U moment contributions based on a dipole approximation. The orbital part of the uranium, μ_L^U, is the leading moment on the uranium site in both single crystals and is parallel to the applied magnetic field. The weaker uranium spin part, μ_S^U, is coupled antiparallel to the μ_L^U. This is the conventional character of the U magnetic moment in many uranium-based compounds[25, 26] including UCoGe[21, 24]. We find that μ_L^U grows faster on account of μ_S^U which is preferably projected in the increase of the $|\mu_L^U/\mu_S^U|$ ratio from the 1.9 to 2.3 for $UCo_{0.97}Ru_{0.03}Ge$ and $UCo_{0.88}Ru_{0.12}Ge$, respectively (Fig. 6).
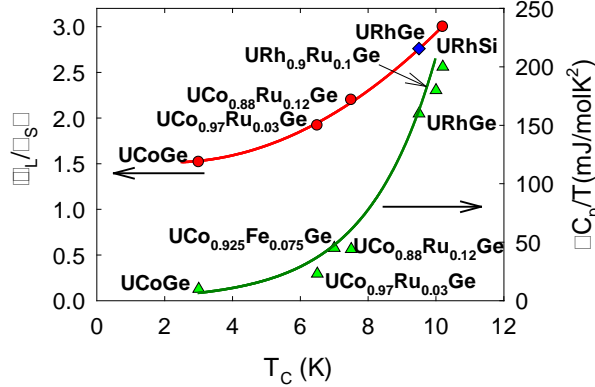

FIG. 6. (Color online) Evolution of the $|\mu_L^U/\mu_S^U|$ ratio and magnitude of heat capacity jumps as $\Delta C_p/T$ in relation to T_C of the TiNiSi-type ferromagnetic UTX compounds. All points of the $|\mu_L^U/\mu_S^U|$ ratios are scaled to external magnetic field of 7 T (URhSi 6T). Blue point suggests the expected value of the $|\mu_L^U/\mu_S^U|$ ratio for the URhGe where experimental data are still missing. The values of $|\mu_L^U/\mu_S^U|$ were calculated from data available in Refs.[21, 25], $\Delta C_p/T$ are taken from Refs.[3, 13, 42]. The solid lines are only to guide the eye.

The value of $|\mu_L^U/\mu_S^U|$ is an important parameter having impact on the hybridization strength of the system. The values of the magnetic moments for free U^{3+} are $\mu_L^{U^{3+}}$ = 5.585 μ_B and $\mu_S^{U^{3+}}$ = -2.169 μ_B; for free U^{4+} $\mu_L^{U^{4+}}$ = 4.716 μ_B and $\mu_S^{U^{4+}}$ = -1.432, which give $|\mu_L^U/\mu_S^U|$ ratio 2.6 for U^{3+} and 3.3 for U^{4+}.[25] It is clear that observed values of μ_L^U and μ_S^U in Table III are far from the free ions values due to strong hybridization with the s, p, d valence states and direct overlap of the 5f wave functions.

Thus, due to significantly reduced values of μ_L^U and μ_S^U in real system it is difficult to estimate the U ion state from the obtained $|\mu_L^U/\mu_S^U|$ values with respect to those expected for free ions. Nevertheless the evolution of the $|\mu_L^U/\mu_S^U|$ ratios is still an important parameter carrying indirect information about the hybridization strength within the selected systems[52]. Generally, a higher value of $|\mu_L^U/\mu_S^U|$ signs localization of 5f electrons because the μ_L^U density in U intermetallics is usually distributed closer to ion center than the spin moment density[53, 54]. For example in ferromagnetic $UAsSe$[55] with localized 5f states the ratio of $|\mu_L^U/\mu_S^U|$ = 3.2, but even here absolute values of and μ_S^U and μ_L^U are far from free ions values. We have rescaled the values of μ_L^U and μ_S^U in UCoGe by a linear extrapolation of the available data[21] up to a magnetic field of 7 T using the formulas μ_L^U = 0.0344μ_0H + 0.0767 and μ_S^U = -0.0211μ_0H - 0.0667, calculated the $|\mu_L^U/\mu_S^U|$ ratio, and plotted it as a function of T_C (see Fig. 6). The original data in magnetic field of 6 T for URhSi are used in Fig. 6. As it is evident from Fig. 6, there is clear growth of the $|\mu_L^U/\mu_S^U|$ ratios from UCoGe toward URhSi. Thus the hybridization strength as delocalization mechanism is the lowest in URhSi where 5f states are much localized within the whole series. $|\mu_L^U/\mu_S^U|$ ratios for Ru substituted UCoGe single crystals are between the UCoGe and URhSi, signalizing that the 5f states are more localized

than in parent UCoGe compound and that the hybridization strength as delocalization mechanism is weaker. However, the low absolute values of μ_L^U and μ_S^U in comparison to UAsSe indicate that UCo$_{0.97}$Ru$_{0.03}$Ge and UCo$_{0.88}$Ru$_{0.12}$Ge and even URhSi can be classified as itinerant ferromagnets[56]. Our finding of a gradual localization of the 5f states in UCo$_{0.97}$Ru$_{0.03}$Ge and UCo$_{0.88}$Ru$_{0.12}$Ge deduced from $|\mu_L^U/\mu_S^U|$ ratios is in a very good agreement with the relevant physical quantities obtained from our macroscopic measurements: We have found systematic scaling of the heat capacity jumps $\Delta C_p/T$ at T_C for TiNiSi-type UTX compounds – see Fig.6. The highest $\Delta C_p/T$ has been found as expected for the URhGe and URhSi. However, proportional magnetic entropy, having similar trend like $\Delta C_p/T$, even in URhSi is very weak suggesting high 5f electron itineracy[56] in agreement with PND data. Consistent with this, the value of S_{mag} of UCoGe (only 3% of RLn2)[3] is very close to zero expected for true weak itinerant ferromagnets[5]. The found scaling of the $\Delta C_p/T$ as a function of T_C is subject of theoretical calculation within the SCR theory[57, 58] and will be published as separated work.

The gradual localization of 5f states is also reflected in the shape of the magnetization loops of UCo$_{0.97}$Ru$_{0.03}$Ge and UCo$_{0.88}$Ru$_{0.12}$Ge which are significantly rectangular than that of parent UCoGe (Fig. 1) and the value of $\mu_{spont.}$ is almost 3 times higher in UCo$_{0.88}$Ru$_{0.12}$Ge compared to that of UCoGe. Nevertheless, magnetic moment of UCo$_{0.88}$Ru$_{0.12}$Ge at 1.8 K and 7 T is still only ≈ 10 % of magnetic moment of free U^{3+} or U^{4+} ion. Also we find that the magnitude of the spin fluctuations is significantly reduced in substituted compounds due to 5f states localization compared to that of UCoGe. This is evident from the behavior of the magnetization along the b-axis which is similarly hard like a-axis magnetization and also from the weaker knee in electrical resistivity data at 40 K along the c-axis compared to that in parent UCoGe[33, 43]. The observed suppression of the ferromagnetic fluctuations in the substituted samples with additional electron-magnon scattering processes is most likely the reason of the immediate disappearance of superconductivity in the substituted systems.

On the basis of our PND data in combination with the macroscopic measurements, we conclude that value of T_C and $\mu_{spont.}$ in TiNiSi-type UTX compounds are determined by the strength of the 5f-d hybridization and the corresponding localization of the 5f states. Our PND results support the scenario of the stabilization of FM via a growth of uranium orbital moment μ_L^U and the consequent localization of the 5f states on U site. This can also be generalized to other FM alloys with TiNiSi-structure like UCo$_{1-x}$Fe$_x$Ge[13], URh$_{1-x}$Co$_x$Ge[59] and URh$_{1-x}$Ru$_x$Ge[17].

Our scenario is supported by the theoretical model proposed by Silva Neto et. al.[65] considering hybridization as a function of varying width and positions of the ligand d- and uranium 5f-band to explain the origin of the observed FM dome in the URh$_{1-x}$Co$_x$Ge. Similar conclusion was also found for URh$_{1-x}$Ru$_x$Ge system by XPS study where enlarged DOS at E_F was found to be due to hybridized 4d-5f band[44]. The XPS data of URh$_{1-x}$Ru$_x$Ge study also explains our observation of the enhanced value of γ coefficient in UCo$_{0.97}$Ru$_{0.03}$Ge and UCo$_{0.88}$Ru$_{0.12}$Ge single crystals where non-Fermi liquid state also develops in the UCo$_{1-x}$Ru$_x$Ge system at x = 0.31%[14].

Finally we would like to discuss and compare the values of the U and Co magnetic moments of our substituted samples with those reported for UCoGe[21]. Generally, the existence of a weak induced parallel moment on the transition metal site is a common feature observed in all other so far studied UTX intermetallic compounds e.g. URhSi[25], UCoAl[26, 27], URhAl[28] or URuAl[29]. In contrast, previous PND study[21] performed on parent UCoGe suggests the existence of a very large Co magnetic moment antiparallel to the uranium moment in high magnetic field. This result is in disagreement with the recent XMCD results reported on UCoGe where parallel U and Co moments where found[30, 60]. $|\mu_L^U/\mu_S^U|$ ratio from the XMCD spectra is almost field independent and of similar magnitude like our substituted

compounds[30]. The previous $|\mu_L^U/\mu_S^U| = 3$ reported for the UCoGe[21] at 0.1 K and 12 T is significantly larger than those of our substituted samples and does not fit to the model presented in Fig. 6. We have extrapolated the values of the μ_L^U, μ_S^U and μ_S^{Co} of the substituted compounds to obtain values for parent UCoGe ($x = 0$) (see Fig.7). The obtained values are $\mu_L^U = 0.17\mu_B$, $\mu_S^U = -0.097\mu_B$ and $\mu_S^{Co} = 0.012\mu_B$ for a magnetic field of 7 T. Especially the value and also the sign of μ_S^{Co} scale well with the data obtained from recent XMCD work[30].
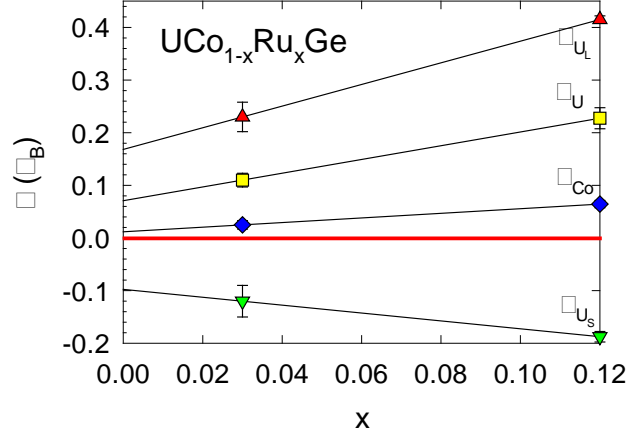

FIG. 7. (Color online) Evolution of all magnetic components in $UCo_{0.97}Ru_{0.03}Ge$ and $UCo_{0.88}Ru_{0.12}Ge$ single crystals. Values from dipolar approximation are used for figure construction. Magnetic components of $UCo_{0.88}Ru_{0.12}Ge$ single crystal are rescaled to magnetic field of 7 T to put it in the same scale with the experimental data of $UCo_{0.97}Ru_{0.03}Ge$.

Considering the fact that the magnetic moment at the cobalt site μ_S^{Co} is predominantly induced by the spin part of uranium moment[61] μ_S^{Co} can be used as a local probe for spin moment at the uranium site. As shown in Table III, μ_S^{Co}/μ_S^U ratios are similar within the experimental accuracy for both substituted compounds, justifying our assumption.

V. Conclusions

We have successfully carried out PND experiments in two Ru substituted UCoGe single crystals to explore the microscopic mechanism of anomalous growth of T_C and μ_{spont} and the observed FM dome in $UCo_{1-x}Ru_xGe$. We have shown that Ru substitution ($x \leq 0.1$)[14] apparently leads to an increase of the U orbital moment μ_L^U (and consequently the total U moment), which reflects certain localization of the 5f electrons as it is manifested by a corresponding growth of the $|\mu_L^U/\mu_S^U|$ ratio. We may conclude that appearance of the FM dome in $UCo_{1-x}Ru_xGe$ is due to a change of the degree of 5f-ligand hybridization which determined the degree of localization of the U 5f states.

Our PND study confirmed that the initial grow of T_C and $\mu_{spont.}$ ($x \leq 0.1$) in $UCo_{1-x}Ru_xGe$ is due to weakness of hybridization strength as delocalization mechanism which supports the scenario suggested in Ref.[14]. Surprising scaling of the $|\mu_L^U/\mu_S^U|$ and heat capacity jumps $\Delta C_p/T$ at T_C (and magnetic entropy S_{mag}) (Fig. 6) allowed us generalization of gradual hybridization strength for all ferromagnetic UTX compounds adopting the orthorhombic TiNiSi–type crystal structure which clearly corroborates the scenario for UCoGe that it is a very weak itinerant ferromagnet with strongly delocalized 5f electrons.

The study has further shown that the most localized 5f electrons within the series are in URhSi and URhGe, even so the localization of the 5f states is still far from typical local moment ferromagnets like UAsSe. The gradual localization of the 5f states in the substituted

compounds is also in very good agreement with the relevant physical quantities obtained from our macroscopic measurements which reflects the gradual reduction of spin fluctuations with increasing x up to 0.12. Magnetization loops are more rectangular with higher $\mu_{\text{spont.}}$, lower high-field susceptibility, higher jumps C_P jumps at T_C. In addition, the associated magnetic entropy S_{mag} in specific heat and also knee at ≈ 40 K in the electrical resistivity can be attributed to a reduction of spin fluctuations with increasing Ru content. The suppressed ferromagnetic fluctuations are probably (besides the substitutional disorder) responsible for the sudden loss of superconductivity in the substituted systems.

The parallel alignment of the U and Co moments observed in $UCo_{0.97}Ru_{0.03}Ge$ and $UCo_{0.88}Ru_{0.12}Ge$ are in accord with the results of the Compton scattering and XMCD experiments on UCoGe at temperatures of the normal ferromagnetic state. Further detailed PND and XMCD studies are necessary to reveal the origin of high field and low temperature magnetic state of UCoGe[21].

Acknowledgements

REFERENCES

[1] S. S. Saxena, et al., Nature **406**, 587 (2000).

[2] D. Aoki, A. Huxley, E. Ressouche, D. Braithwaite, J. Flouquet, J. P. Brison, E. Lhotel, and C. Paulsen, Nature **413**, 613 (2001).

[3] N. T. Huy, et al., Physical Review Letters **99**, 067006 (2007).

[4] H.H.Hill, Plutonium, A. Other, and N. Y. Aime, AIME,New York, 2 (1970).

[5] V. Sechovsky and L. Havela, in *Handbook of Magnetic Materials*, edited by K. H. J. Buschow (Elsevier, 1998), Vol. Volume 11, p. 1.

[6] N. Tateiwa, Y. Haga, T. D. Matsuda, E. Yamamoto, and Z. Fisk, Physical Review B **89**, 064420 (2014).

[7] F. Hardy, A. Huxley, J. Flouquet, B. Salce, G. Knebel, D. Braithwaite, D. Aoki, M. Uhlarz, and C. Pfleiderer, Physica B-Condensed Matter **359**, 1111 (2005).

[8] S. Sakarya, N. H. van Dijk, A. de Visser, and E. Brück, Physical Review B **67**, 144407 (2003).

[9] E. Slooten, T. Naka, A. Gasparini, Y. K. Huang, and A. de Visser, Physical Review Letters **103**, 097003 (2009).

[10] E. Hassinger, D. Aoki, G. Knebel, and J. Flouquet, Journal of the Physical Society of Japan **77**, 073703 (2008).

[11] J. Pospisil, J. P. Vejpravova, M. Divis, and V. Sechovsky, Journal of Applied Physics **105**, 07E114 (2009).

[12] J. J. Hamlin, R. E. Baumbach, K. Huang, M. Janoschek, N. Anchanavatee, and D. A. Zocco, Mater.Res.Soc.Symp.Proc. **1264**, 1264 (2010).

[13] K. Huang, J. J. Hamlin, R. E. Baumbach, M. Janoschek, N. Kanchanavatee, D. A. Zocco, F. Ronning, and M. B. Maple, Physical Review B **87**, 054513 (2013).

[14]   M. Valiska, J. Pospisil, V. Sechovsky, and M. Divis, arXiv:1412.8355 [cond-mat.str-el] (2014).

[15]   S. Sakarya, N. H. van Dijk, N. T. Huy, and A. de Visser, Physica B-Condensed Matter **378-80**, 970 (2006).

[16]   S. Sakarya, et al., Journal of Alloys and Compounds **457**, 51 (2008).

[17]   N. T. Huy, A. Gasparini, J. C. P. Klaasse, A. de Visser, S. Sakarya, and N. H. van Dijk, Physical Review B **75**, 212405 (2007).

[18]   D. Aoki, I. Sheikin, T. D. Matsuda, V. Taufour, G. Knebel, and J. Flouquet, Journal of the Physical Society of Japan **80**, 013705 (2011).

[19]   T. V. Bay, A. M. Nikitin, T. Naka, A. McCollam, Y. K. Huang, and A. de Visser, Physical Review B **89**, 214512 (2014).

[20]   W. Knafo, et al., Physical Review B **86**, 184416 (2012).

[21]   K. Prokes, A. de Visser, Y. K. Huang, B. Fak, and E. Ressouche, Physical Review B **81**, 180407R (2010).

[22]   E. Steven, A. Kiswandhi, D. Krstovska, J. Brooks, M. Almeida, A. Goncalves, M. Henriques, G. Luke, and T. Williams, Applied Physics Letters **98**, 132507 (2011).

[23]   M. Divis, Physica B-Condensed Matter **403**, 2505 (2008).

[24]   J. Taylor, J. Duffy, M. Butchers, C. Stock, and E. Bauer, Bulletin of the American Physical Society **56**, Z25.9 (2011).

[25]   K. Prokes and A. Gukasov, Physical Review B **79**, 024406 (2009).

[26]   P. Javorsky, V. Sechovsky, J. Schweizer, F. Bourdarot, E. Lelievre-Berna, A. V. Andreev, and Y. Shiokawa, Physical Review B **63**, 064423 (2001).

[27]   Y. Takeda, Y. Saitoh, T. Okane, H. Yamagami, T. D. Matsuda, E. Yamamoto, Y. Haga, Y. Onuki, and Z. Fisk, Physical Review B **88**, 075108 (2013).

[28]   J. A. Paixão, G. H. Lander, P. J. Brown, H. Nakotte, F. R. de Boer, and E. Brück, Journal of Physics-Condensed Matter **4**, 829 (1992).

[29]   J. A. Paixão, G. H. Lander, A. Delapalme, H. Nakotte, F. R. de Boer, and E. Brück, Europhysics Letters **24**, 607 (1993).

[30]   M. Taupin, J. P. Brison, D. Aoki, L.-P. Sanchez, F. Wilhelm, and A. Rogalev, arXiv:1501.01251 [cond-mat.str-el] (2015).

[31]   M. Taupin, L. Howald, D. Aoki, J. Flouquet, and J. P. Brison, Physical Review B **89**, 041108(R) (2014).

[32]   M. Valiska, J. Pospisil, G. Nenert, A. Stunault, K. Prokes, and V. Sechovsky, JPS Conf. Proc. **3**, 012011 (2014).

[33]   J. Pospisil, K. Prokes, M. Reehuis, M. Tovar, J. P. Vejpravova, J. Prokleska, and V. Sechovsky, Journal of the Physical Society of Japan **80**, 084709 (2011).

[34]   N. T. Huy, Y. K. Huang, and A. de Visser, Journal of Magnetism and Magnetic Materials **321**, 2691 (2009).

[35]   H. Rietveld, Journal of Applied Crystallography **2**, 65 (1969).

[36]   J. Rodriguez-Carvajal, Physica B: Condensed Matter **192**, 55 (1993).

[37]   T. Roisnel and J. Rodriguez-Carvajal, in *EPDIC 7 - Seventh European Powder Diffraction Conference*, edited by R. Delhez and E. J. Mittemeijer (Trans Tech Publications, Barcelona, Spain, 2000).

[38]   E. Lelievre-Berna, et al., Physica B-Condensed Matter **356**, 141 (2005).

[39]   Y. Saitoh, et al., Journal of Synchrotron Radiation **19**, 388 (2012).

[40]   A. Arrott, Physical Review **108**, 1394 (1957).

[41]   K. Prokes, et al., Physica B: Condensed Matter **311**, 220 (2002).

[42]   K. Prokes, T. Wand, A. V. Andreev, M. Meissner, F. Honda, and V. Sechovsky, Journal of Alloys and Compounds **460**, 47 (2008).

[43] T. Hattori, Y. Ihara, K. Karube, D. Sugimoto, K. Ishida, K. Deguchi, N. K. Sato, and T. Yamamura, Journal of the Physical Society of Japan **83**, 061012 (2014).

[44] V. H. Tran, A. Slebarski, and W. Müller, Journal of Alloys and Compounds **451**, 497 (2008).

[45] F. Canepa, P. Manfrinetti, M. Pani, and A. Palenzona, Journal of Alloys and Compounds **234**, 225 (1996).

[46] *Maximum Entropy and Bayesian Methods* (Kluwer, Dordrecht, 1989).

[47] S. F. Gull and J. Skilling, *MEMSYS III Quantified Maximum Entropy Subroutine Library* (Meldreth, UK, 1989).

[48] R. J. Papoular and B. Gillon, Europhysics Letters **13**, 429 (1990).

[49] G. H. Lander, M. S. S. Brooks, and B. Johansson, Physical Review B **43**, 13672 (1991).

[50] B. T. Thole, P. Carra, F. Sette, and G. Vanderlaan, Physical Review Letters **68**, 1943 (1992).

[51] P. Carra, B. T. Thole, M. Altarelli, and X. D. Wang, Physical Review Letters **70**, 694 (1993).

[52] K. Kaneko, N. Metoki, N. Bernhoeft, G. H. Lander, Y. Ishii, S. Ikeda, Y. Tokiwa, Y. Haga, and Y. Onuki, Physical Review B **68**, 214419 (2003).

[53] O. Eriksson, M. S. S. Brooks, and B. Johansson, Physical Review B **41**, 9087 (1990).

[54] M. Wulff, G. H. Lander, B. Lebech, and A. Delapalme, Physical Review B **39**, 4719 (1989).

[55] P. Wisniewski, A. Gukasov, Z. Henkie, and A. Wojakowski, Journal of Physics-Condensed Matter **11**, 6311 (1999).

[56] K. Prokes, T. Wand, A. V. Andreev, M. Meissner, F. Honda, and V. Sechovsky, Journal of Alloys and Compounds **460**, 47 (2008).

[57] P. Mohn and G. Hilscher, Physical Review B **40**, 9126 (1989).

[58] T. Moriya, Journal of Magnetism and Magnetic Materials **14**, 1 (1979).

[59] N. T. Huy and A. de Visser, Solid State Communications **149**, 703 (2009).

[60] M. Taupin, Ph.D. thesis, Universite Joseph-Fourier, 2013.

[61] M. S. S. Brooks, O. Eriksson, and B. Johansson, Journal of Physics-Condensed Matter **1**, 5861 (1989).